CFD Letters www.cfdl.issres.net Vol. 4 (4) – December 2012

Computations of Upward Water/Air Fluid Flow in Vertical Pipes

I.M. Sakr*, W.A. El-Askary, A. Balabel, K. Ibrahim

Mechnical Power Engineering Dept., Faculty of Engineering,
Menoufia University, Shebin El-Kom, EGYPT.

Received: 27/06/2012 – Revised 25/11/2012 – Accepted 02/12/2012

Abstract

In the present paper, a numerical code has been developed with different turbulence models aiming at simulating turbulent bubbly flows in vertical circular pipes. The mass and momentum conservation equations are used to describe the motion of both phases (water/air). Because of the averaging process additional models are needed for the inter-phase momentum transfer and turbulence quantities for closure. The continuous phase (water) turbulence is represented using different turbulence models namely: two-equation k-ε, extended k-ε and shear-stress transport (SST) k-ω turbulence models which contains additional term to account for the effect of the dispersed phase (air) on the continuous phase turbulence. The developed code is based on the finite volume method with the mentioned different turbulence models. The Reynolds stresses of the dispersed phase are calculated by relating them to those of the continuous phase through a turbulence response function. The code has been tested through two different cases: the prediction of air/water bubbly flow in a vertical pipe and bubbly flow in a sudden enlargement pipe where phase fractions, velocity profiles and turbulence can be compared with available experimental data. It is concluded that, SST k-ω produces the best validations in view with the other turbulence models and the comparisons with other simulations and experimental data from literature.

Keywords: Two-phase flow; Eulerian model; turbulence models; SST model

1. Introduction

Two-phase flows have significant importance in many industrial applications. Some of these applications includes boiling heat transfer, cloud cavitations in hydraulic systems, stirring of reactors, aeration in water purification, bubble columns and centrifuges in the petrochemical industry, cooling devices of nuclear reactors and electrochemical reaction. Among others, bubbly flows have a great importance in the electrochemical reaction and particularly in hydrogen production, chlorate process, electroplating and metal purification processes [1-2]. Bubbly flows consist of gas bubbles (dispersed phase) within a carrier liquid (continuous phase). Among several two phase flow models, there are two fundamentally different formulations of the microscopic field equations for two phase flow systems; namely the Eulerian two fluid model. In two-fluid model, each phase is separately described in terms of two sets of conservation equations. Knowledge of the characteristics of bubbly flows is important in the design of multi-fluid system. As the

* Corresponding Author: Ismail Sakr
Email: ismailsakr@yahoo.com Telephone: +2-048-2333081 Fax: +2-048-2235695
 PII: S2180-1363(12)4193-X

computer power dramatically increases each year, it is desirable to employ advanced multi-dimensional models to calculate bubbly flows more precisely through methods of computational fluid dynamics (CFD).

These models should be able to account for such effects as turbulence, strong interaction between phases and multi-dimensionality, which are the general attributes of the most of bubbly flows. The model should also rely on the empirical data to the least possible extent. In spite of the progress achieved in the development of Eulerian-Eulerian, two–fluid models for bubbly flows, (Simonin and Viollet [3]; Lee et.al. [4]; Lopez de Bertodano et al. [5]; Bel Fdhila and Simonin, [6]; Lopez de Bertodano et al., [7]), some important difficulties subsist.

Lopez de Bertodano [8] used two-phase extension of the algebraic stress model (ASM) to model turbulence effects in the liquid phase. The turbulence scale equations were derived on the presumption that the total liquid turbulence is a sum of shear and the bubble induced components. Total liquid eddy diffusivity was modified by an addition of the bubble-induced eddy diffusivity introduced by Sato et al. [9]. A comparison of this model's prediction with experimental data on bubbly flows, in a vertical duct, gave encouraging result. Wang et al. [10] investigated turbulent bubbly air/water flows using a pipe in which both up and down flows were investigated. Flow parameters such as void fraction, liquid velocity and turbulence intensity were measured in fully developed flow conditions for both up and down flows. Troshko and Hassan [11] derived a new wall law for two phase flows in Eulerian–Eulerian frame and tested its validity in bubbly flows using CFX. Bubbly upflow in a sudden expansion was analyzed with a two-fluid model in a circular cross section pipe. For such flows the presence of the interfacial drag force in the momentum equations introduces source terms into the transport equations for both the turbulence kinetic energy and its dissipation rate. These source terms were first identified by Gosman et. al. [12].The experiment of Bel F'dhila and Simonin [6] and Bel F'dhila [13] includes investigations of turbulent concurrent bubbly upward flow through a sudden area expansion. This experiment is important because of the specific flow conditions developed: high level of turbulence and strong shear stresses with significant adverse pressure gradients. Behzadi et al [14] used an in–house CFD to study bubbly flows in a sudden pipe expansion. Eulerian-Eulerian approach with $k-\varepsilon$ model was used to model the multiphase and turbulence in the domain respectively. Carver [15] reviewed the various approaches for constructing a void fraction algorithm. Carver [15] first recommended normalizing each mass conservation equation by its own reference density and then summing the two equations to form an equation that will be used to determine the pressure correction. The two normalized mass conservation equations are then subtracted to develop the equation for determining the void fraction. Issa and Oliveira [16] investigated turbulent bubbly air/water flows in a sudden expansion using Eulerian-Eulerian model. They obtained volume fraction by two method: the first method (Standard method); solve the continuity equation of dispersed phase and the continuous phase volume fraction is obtained from equation ($\alpha_c = 1-\alpha_d$). The second method, volume fraction for each phase is computed separately from their mass conservation equation. Manmatha and Sukasnta [17] investigated theoretical studies to determine the pressure drops caused by abrupt flow area expansion/contraction in small circular pipes for two-phase flow of air/water mixture at room temperature and near to atmospheric pressure.

The main objective of the present work is to develop a numerical code to simulate the turbulent bubbly flow either in a vertical straight or in a vertical sudden enlargement pipes. Two-fluid model of adiabatic, incompressible bubbly flows is described with an emphasis on all important interfacial forces. Three turbulent models; the standard $k-\varepsilon$ (STD) model, the extended $k-\varepsilon$ (ETD) model and the shear-stress transport (SST) k-ω model are implemented in this code, in which the last model was not previously considered in the literature for simulating the bubbly flow. The computation results are compared with available experimental data and with previous computation results.

2. Mathematical Model

2.1. Governing equations

In the present work, the two-fluid model (Eulerian-Eulerian model) has been used. In the Euler-Euler approach, the different phases are treated mathematically as interpenetrating continua, with each computational cell of the domain containing respective fractions of the continuous and dispersed phases. The model assumptions are:

1-The fluids in both phases are Newtonian, viscous and incompressible.

2-The physical properties remain constant.
3-The pressure is assumed to common to both phases.
4-Surface tension effect is neglected.
5-The different turbulence models are used to describe the behavior of the continuous phase.
6-The flow is assumed to be isothermal, so energy equation is not needed.
With all the above assumptions the governing equations for phase k (c for continuous and d for dispersed) can be written as [13, 14, 16, and 17]:
The continuity equation:

$$\frac{\partial}{\partial x_i}(\alpha\rho u_i)_k = 0.0 \tag{1}$$

The volume fractions are assumed to be continuous functions of space and time and their sum is equal to one.

$$\alpha_c + \alpha_d = 1.0 \tag{2}$$

RANS equations:

$$\frac{\partial}{\partial x_j}(\alpha\rho u_i u_j)_k = -\alpha\frac{\partial p}{\partial x_i} + \frac{\partial}{\partial x_j}\left[\alpha\mu\left(\frac{\partial u_i}{\partial x_j} + \frac{\partial u_j}{\partial x_i} - \frac{2}{3}\delta_{ij}\frac{\partial u_l}{\partial x_l}\right)\right]_k + \frac{\partial}{\partial x_j}(-\rho u_i' u_j')_k \pm M_k \tag{3}$$

where u denotes mean velocities and u` is the fluctuating or turbulence velocity, ρ is density, p is pressure, M_k is the interface momentum transfer term and μ is the laminar viscosity. The additional fluctuating quantities are known as the Reynolds stresses, which must be modeled in order to close the system of equations. The apparent turbulent shearing stresses might be related to the rate of mean strain through an apparent scalar turbulent or "eddy" viscosity. For the general Reynolds stress tensor, the Boussinesq assumption reads:

$$-\rho u_i' u_j' = \mu_t\left(\frac{\partial u_i}{\partial x_j} + \frac{\partial u_j}{\partial x_i}\right) - \frac{2}{3}\left(\rho k + \mu_t\frac{\partial u_k}{\partial x_k}\right)\delta_{ij} \tag{4}$$

where δ_{ij} is the Kronecker delta function (δ_{ij} =1 if i=j and δ_{ij} =0 if i≠j), k is the turbulent kinetic energy and μ_t is the turbulent viscosity, which can be computed from the suitable turbulence model.
The interface momentum transfer term Mk is given in Troshko and Hassan [11]

$$M_c = M_c^d + M_c^L + M_c^W + M_c^{td} \tag{5}$$

where the individual terms on the right-hand side of Equation (5) are the drag force (M_c^d), lift force(M_c^L), wall force(M_c^W) and turbulent dispersion force (M_c^{td}), respectively. The drag force is expressed as [11]

$$M_c^d = -M_d^d = \frac{3}{4}\frac{C_D}{d_b}\alpha_d\alpha_c\left|u_d - u_c\right|(u_d - u_c) \tag{6}$$

In which the drag coefficient C_D depends on the particle Reynolds number as given below [18, 19]:

$$C_D = \begin{cases}\dfrac{24}{R_e}(1 + 0.15R_e^{0.687}), \mathrm{Re} \le 1000\\ 0.44 \qquad\qquad \mathrm{Re} > 1000\end{cases} \tag{7}$$

Relative Reynolds number is given by

$$\mathrm{Re} = \frac{\rho_c\left|u_d - u_c\right|d_b}{\mu_c} \tag{8}$$

Equation (5) shows that the drag force exerted by the secondary phase (bubbles) on the primary phase is a vector directed along the relative velocity of the secondary phase.
The second term in Equation (5) represents the lift force, which arises from a velocity gradient of the continuous phase as given by [11]:

$$M_c^L = -M_d^L = C_L \alpha_c \alpha_d \rho_c (u_d - u_c) \times (\nabla \times u_c) \tag{9}$$

where C_L is the lift force coefficient. The value of the lift coefficient ranges from 0.01 for the laminar flow to 0.5 for the inviscid flow around the sphere. Troshko and Hassan [11] recommended C_L =0.06 for turbulent bubbly flows in vertical pipes.
The wall lubrication force is first presented by Antal and Lahey [20]. They defined an analytical expression for a wall force that prevents the bubbles from touching the wall. The main effect of the wall force is to assure the zero void condition found experimentally near vertical walls while not significantly affecting the phase distribution away from the wall. The wall lubrication force is defined as:

$$M_c^W = -M_d^W = \frac{\alpha_c \alpha_d \rho_c \left| u_d - u_c \right|}{d_b} \max(0, C_{w1} + C_{w2} \frac{d}{y_w}) n_w \tag{10}$$

Where n_w the outward unit vector is perpendicular to the wall and y_w is the distance from that wall to the bubble. The constants C_{w1} and C_{w2} determine the magnitude and the effective action distance which is equal to dC_{w2} / C_{w1}.
The turbulent dispersion force, derived by Lopez de Bertodano [8], is based on the analogy with molecular movement. It approximates a turbulent diffusion of the bubbles by the liquid eddies. It is formulated as:

$$M_c^{td} = -M_d^{td} = -C_{td} \rho_c k_c \nabla \alpha_c \tag{11}$$

Where k_c is the liquid turbulence kinetic energy per unit mass. Lopez de Bertodano [8] suggested the value of the coefficient C_{td} to be of order 0.09 to 0.1.

2.2. Turbulence modeling

Three different turbulence models are included in the numerical code. The correct selection of the suitable model is dependent on a combination of accuracy and acceptable computational time. In the present paper, the turbulence models are tested and evaluated for the case considered; namely: the standard k-ε (STD) model [12, 16], the extended k-ε (ETD) model [21] and the shear-stress transport (SST) k-ω model [22, 23, and 24]. The general transport equations for the adopted models are given below, while the different terms and coefficient of the turbulence models adopted are given in Table 1.
The k-equation:

$$\frac{\partial}{\partial x_j}(\alpha \rho u k)_k = \frac{\partial}{\partial x_j}\left[(\mu + \frac{\mu_t}{\sigma_k}) \frac{\partial k}{\partial x_j} \right]_k + \rho \alpha (P_k^* - \beta_1 \varepsilon - \beta_2 k \omega)_k + S_k^{\text{int}} \tag{12}$$

The ε-equation:

$$\frac{\partial}{\partial x_j}(\alpha \rho u \varepsilon)_k = \frac{\partial}{\partial x_j}\left[(\mu + \frac{\mu_t}{\sigma_\varepsilon}) \frac{\partial \varepsilon}{\partial x_j} \right]_k + \rho \alpha \frac{\varepsilon}{k} (C_{\varepsilon 1} P_k - C_{\varepsilon 2} \varepsilon + \frac{C_{\varepsilon 3} P_k^2}{\varepsilon})_k + S_\varepsilon^{\text{int}} \tag{13}$$

The ω-equation:

$$\frac{\partial}{\partial x_j}(\alpha\rho u\,\omega)_k = \frac{\partial}{\partial x_j}\left[(\mu+\frac{\mu_t}{\sigma_\omega})\frac{\partial\omega}{\partial x_j}\right]_k + \left[\rho\alpha\alpha_3\frac{\omega}{k}P_k\right]_k - \left(\alpha\rho\beta_3\omega^2\right)_k + (1.7123\alpha\rho(1-F_1)\nabla k\,\nabla\omega)_k + S_\omega^{\text{int}} \quad (14)$$

TABLE 1: COEFFICIENT FOR TURBULENCE MODELS

	STD $k-\varepsilon$ model	ETD $k-\varepsilon$ model	SST $k-\omega$
β_1	1	1	0
β_2	0	0	0.09
β_3	0	0	$0.075F_1+0.0828(1-F_1)$
σ_k	1	0.75	$1.176F_1+(1-F_1)$
σ_ε	1.3	1.15	0
σ_ω	0	0	$2F_1+1.168(1-F_1)$
P_k	$2\nu_t S_{ij}S_{ij}$	$2\nu_t S_{ij}S_{ij}$	$2\nu_t S_{ij}S_{ij}$
P_k^*	P_k	P_k	$Min(P_k, 10\beta_1\alpha\rho\omega k)$
$C_{\varepsilon 1}$	1.4	1.15	0
$C_{\varepsilon 2}$	1.92	1.9	0
$C_{\varepsilon 3}$	0	0.25	0
μ_t	$\rho C_\mu k^2/\varepsilon$	$\rho C_\mu k^2/\varepsilon$	$0.31\rho k/Max(0.31\omega, F_2(2S_{ij}S_{ij})^{0.5})$
C_μ	0.09	0.09	0
F_1	0	0	$\tanh(\arg_1^4)$
F_2	0	0	$\tanh(\arg_2^2)$
α_3	0	0	$0.56F_1+0.44(1-F_1)$
$\arg_1$	0	0	$\min\left[\max(\frac{\sqrt{k}}{0.09\omega y}, \frac{500\nu}{\omega y^2}), \frac{3.424\rho k}{CD_{kw}y^2}\right]$
$\arg_2$	0	0	$\max\left[2\frac{\sqrt{k}}{0.09\omega y}, \frac{500\nu}{y^2\omega}\right]$

Where y is the distance to the next surface

2.3. Interface turbulent momentum transfer

The source terms accounting for the presence of a dispersed phase and its influence upon the continuous phase turbulence appear in S_k^{int}, $S_\varepsilon^{\text{int}}$ and S_ω^{int}. The source terms are given in Table 2.

TABLE 2: INTERFACE TURBULENT MOMENTUM TRANSFER OF TURBULENCE MODELS

	STD κ-ε model	ETD κ-ε model	SST κ-ω
S_k^{int}	$2k\alpha_c\alpha_d C_D(C_t-1)+ C_D\frac{\nu_t}{\sigma_\alpha}\nabla\alpha(u_d-u_c)$	**0**	**0**
$S_\varepsilon^{\text{int}}$	**0**	$2C_3C_D\alpha_c\alpha_d(C_t-1)\varepsilon$	**0**
S_ω^{int}	**0**	**0**	$2C_3C_D\alpha_c\alpha_d(C_t-1)\beta_2\omega k$

In these turbulent modulation terms, the most important contribution is related to turbulent response coefficient C_t defined as the ratio of the dispersed phase velocity fluctuations to those of the continuous phase $C_t=\frac{u_d'}{u_c'}$. In a related work, a model for C_t was proposed in Ref. [16] to relate C_t to the local flow and turbulence field and was implemented in Ref. [25] in calculation of dilute dispersed flows. The model is given by

$$C_t=\frac{3+\beta}{1+\beta+2\rho_d/\rho_c},\qquad \beta=\frac{t_\varepsilon}{t_p}(1+2\frac{\rho_d}{\rho_c}) \tag{15}$$

Where tε is a time scale of the large eddies (typically $t_\varepsilon=C_4k/\varepsilon$ with C_4 changes between 0.2 to 0.4 [16]) and t_p is the particle relaxation time ($t_p=\left(\frac{\rho_d}{C_D}\right)(1+C_{vm}\rho_c/\rho_d)$ with C_{vm}=0.5, see in Ref. [16]).

The dispersed turbulence kinetic energy and viscosity are related to the continuous phase one by means of response functions:

$$k_d=C_t^2k_c \quad \text{and} \quad \mu_d^t=\frac{\rho_d}{\rho_c}C_t^2\mu_c^t \tag{16}$$

Recent experimental data by Garnier et al. [26] and Larue de Tournemine et al. [27] for gas–liquid flows as well as Augier [28] for liquid–liquid flows suggest that the turbulence response coefficient is a strong function of the phase fraction and that beyond a certain value of α_d which could be as small as 6%, the turbulence response function C_t approaches unity. From experiments given by [14], to account for this effect, a correlation for the turbulence response coefficient as a function of phase fraction was suggested. The correlation was plotted and takes the form as given in Ref. [14].

$$\begin{aligned} C_t&=1+(C_{to}-1)e^{-f(\alpha_d)}\\ f(\alpha_d)&=180\alpha_d-4.71\times10^3\alpha_d^2+4.26\times10^4\alpha_d^4\end{aligned} \tag{17}$$

Where $C_{to}=C_t$ stands for the value of C_t at $\alpha_d\approx0.0$ given in Eq. (15)

2.4. Boundary conditions

The computational domain and boundary conditions are shown in Fig.1. Bubbly vertical pipe flow parameters measured by Wang et al. [10] was first chosen for validation as shown in Fig.1-a. In their experiments, incompressible, air/water bubbly flows at atmospheric pressure

and room temperature were considered. Table 3 shows the global flow condition for each experiment, where J denotes superficial velocity.

TABLE 3: GLOBAL FLOW CONDITIONS OF WANG ET AL. [10] AND BEL F'DHILA ET AL. [6, 10] EXPERIMENTAL.

Case	J_c^{in} (m/s)	J_d^{in} (m/s)	α_d	d (mm)
W1 (pipe)	0.43	0.1	0.132	2.8
W2 (pipe)	0.43	0.27	0.310	3.0
W3 (pipe)	0.43	0.4	0.383	3.2
Bel.(sudden expansion)	1.413	0.181	0.1	2

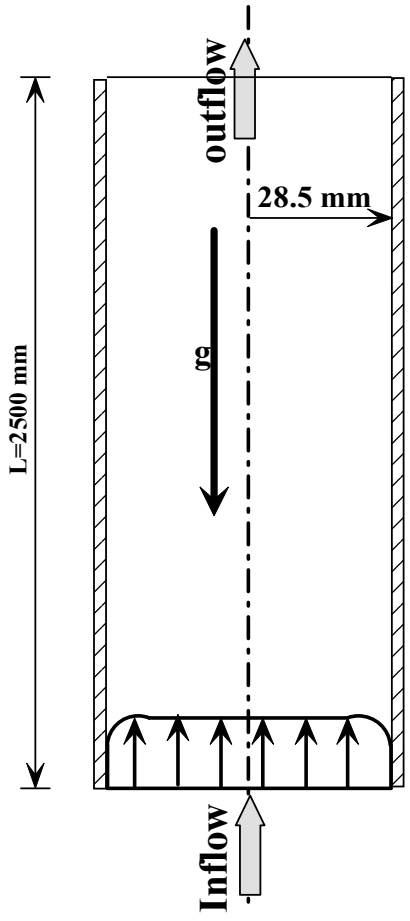

Figure 1(a) Pipe flow (geometry and boundary conditions)

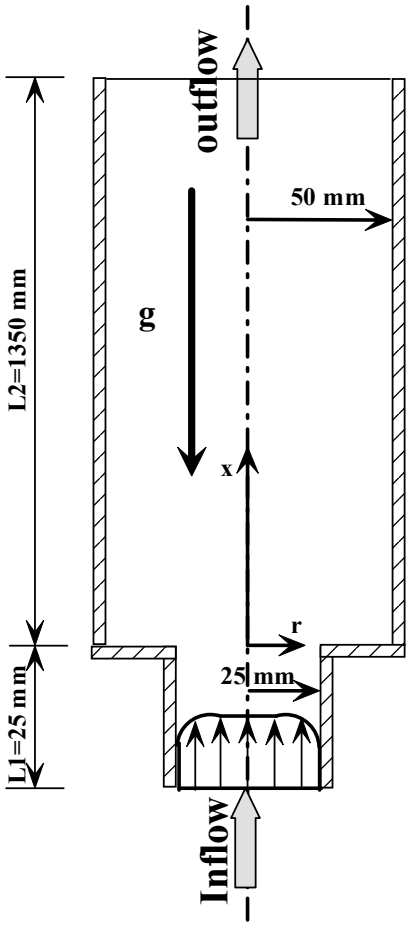

Figure 1(b) Sudden expansion (geometry and boundary conditions)

The models have also been applied to predict bubbly flow in a sudden expansion of a circular pipe is shown in Fig.1-b. Measurements for this test case have been conducted by Bel F'dhila [13] and are presented in Bel F'dhila el al. [6] and Lance et al. [29].The configuration consists of a bubbly air/water flow through a sudden expansion circular pipe. In the experiments, the profiles of mean and RMS velocities (axial and radial components) and of the phase fraction were measured at six cross-sections(x=-2, 7, 13, 18, 25 and 35 cm), measured from the step wall. The Reynolds number based on the smaller pipe diameter and the mean liquid velocity is Re=78500 and the bubble diameter is estimated as d=2 mm and is assume to

be uniform at the entrance section. No-slip boundary conditions are imposed along the wall. The inlet velocity profile is considered to be 1/7-th-power law. The inflow turbulence kinetic energy and its dissipation rate appropriate for fully developed flow in a pipe [30] are assumed

$$k_{in} = k_o(1+4(r/R)^{2.5}) \qquad (18)$$

$$k_o = 0.003U_{in}^2$$

$$\varepsilon_{in} = C_\mu^{0.75} k^{1.5} / \ell_m \qquad (19)$$

The mixing length ℓ_m is given as in [30]:

$$\ell_m = R\left[0.14 - 0.08(1-\frac{y}{R})^2 - 0.06(1-\frac{y}{R})^4\right] \qquad (20)$$

Where R is the radius of the pipe and r is the local radius.
The normal gradients at the outlet plane are taken to be zero except the streamwise velocity, which must be corrected every iteration step to satisfy the continuity equation.

3. Numerical solution

The average transport equations for momentum and mass of each phase as well as for the turbulent in symmetrical flow can be written for steady, incompressible, two-dimensional flows in the following general transport equation form:

$$\nabla.(\alpha\rho u\varphi) = -\alpha\nabla p + \nabla.\left[\alpha\Gamma_\varphi \nabla\varphi\right] + S_\varphi \qquad (21)$$

TABLE 4: GOVERNING EQUATIONS OF LIQUID AND GAS PHASE.

Conservation of	ϕ		S_ϕ
Mass	1	0.0	0.0
Axial momentum	U_k	μ_{eff}	$-\frac{\partial\alpha p}{\partial x} + \frac{\partial}{\partial x}\left(\alpha\mu_{eff}\left(\frac{\partial U_k}{\partial x}\right)\right) + \frac{1}{r}\frac{\partial}{\partial r}\left(\alpha r\mu_{eff}\frac{\partial V_k}{\partial x}\right) \pm M_k$
Radial momentum	V_k	μ_{eff}	$-\frac{\partial\alpha p}{\partial r} + \frac{\partial}{\partial x}\left(\alpha\mu_{eff}\frac{\partial U_k}{\partial r}\right) + \frac{1}{r}\frac{\partial}{\partial r}\left(\alpha\mu_{eff}\left(r\frac{\partial V_k}{\partial r}\right)\right)$ $-2\alpha\mu_{eff}\frac{V_k}{r^2} \pm M_k + g\alpha(\rho_k - \rho)$
Turbulent kinetic energy	k	$\frac{\mu_{eff}}{\sigma_k}$	$\alpha(P-\rho\varepsilon) + S_k^{\text{int}}$
Dissipation rate	ε	$\frac{\mu_{eff}}{\sigma_\varepsilon}$	$\alpha\frac{\varepsilon}{k}\left(C_{\varepsilon 1}f_1 P - C_{\varepsilon 2}f_2\rho\varepsilon\right) + C_3\frac{P^2}{\rho_g k} + S_\varepsilon^{\text{int}}$
Dissipation frequency	ω	$\frac{\mu_{eff}}{\sigma_\omega}$	$\alpha\rho\alpha_3\frac{\omega}{k}P - \alpha\rho\beta_3\omega^2 + (1.7123\alpha\rho(1-F_1)\nabla k\nabla\omega + S_\omega^{\text{int}}$

Where the variable; φ is the dependent variable, representing the streamwise velocity U the normal velocity V, the turbulence kinetic energy k, dissipation rate ε or the dissipation frequency ω, respectively. The diffusion coefficient Γ_φ and source term S_φ in the respective governing equation are specific to a particular meaning of φ, see Table 4.
The numerical method employed here to solve the above general differential equation is based on a general method for prediction of heat and mass transfer, fluid flow and related processes.

This method has been developed and proved its generality and capability in a wide range of possible applications for predicting physically meaningful solutions even for uniform grid [31]. The control volume integration of the above general differential equation, Eq. (21), yields a discretized form being solved numerically on a staggered grid system. The governing equations are discretized using the first-order upwind scheme to achieve the best accuracy. In this paper the SIMPLE algorithm is employed. The algorithm is started with the solution of the discretized momentum equations according to the associated boundary and initial conditions. A pressure correction equation, derived from the integration of the two continuity equations summing (dispersed and continuous phases), are then solved and the solution is used to update the guessed pressure and velocity fields. The other discretized transport equations are then solved. The volume fractions are obtained from solution of one of the continuity equations (dispersed phase) (1). The important question is how to ensure boundedness of α, i.e. $0 \le \alpha \le 1$ for k =c or d. Early studies of this issue are found in Carver [15]. Higher order methods are also possible, and in fact are desirable to improve the accuracy of the predicted volume fraction field and alleviate the problems introduced by the numerical diffusion associated with upwinding. The flow diagram is further iterated until the convergence is achieved in the order of 10^{-3} in velocities, 10^{-4} in pressure and of 10^{-4} in void fraction. The numerical accuracy of the solution is verified by carrying out an appropriate grid refinement study for the test case outlined in the next section. Here, meshes 42×520 and of 82×520 which yields almost identical results are used.

4. Results

The present developed code is verified through test cases. The upward bubbly flow through two different geometries; a vertical straight pipe and a vertical pipe with sudden enlargement. Comparisons with the available measurements against published numerical data will be represented in the following subsections.

4.1. Bubbly flow in a vertical pipe

The velocity profiles, void fraction and turbulence stresses for cases W1, W2 and W3 are presented in Figs. 2, 3 and 4, respectively.

Fig. 2 (a) shows that the void fraction and liquid velocity radial profile are well predicted using the present developed code using the standard k-ε model as well as SST-k-ω model. The other computations of [11] using CFX and PHOENICS codes including the turbulence model of standard k-ε model are also included. Figures 2. (b and c) display the predicted off-diagonal (shear) Reynolds stress of liquid and turbulence scale. The comparisons include also the CFD results in Troshko and Hassan [11]. The Reynolds shear-stress profile indicates that turbulence dominates the central half of the pipe, while bubble pseudoturbulence dominates the wall region, causing a peak in the shears stresses coinciding with the location of the void fraction maximum. However, the quality of the present computations for such case (W1) with low gas flux is not good in view of the other computations. As shown in Fig. 2 (c) the predicted turbulence intensity is in a qualitative agreement with experiments. Experiments W2 and W3 (see Table 3) are also used at higher gas flux conditions to verify the computation. The small deviations are due to the assumed inflow turbulence kinetic energy, dissipation rate and frequency which are not available in the experiment. Figures 3 and 4 display the results of comparison with other computations given by Troshko and Hassan [11]. The predicted void fraction and liquid velocity profiles agreed well with experimental data for both W2 and W3 cases as shown in Figs. 3. (a) and 4(a) respectively.

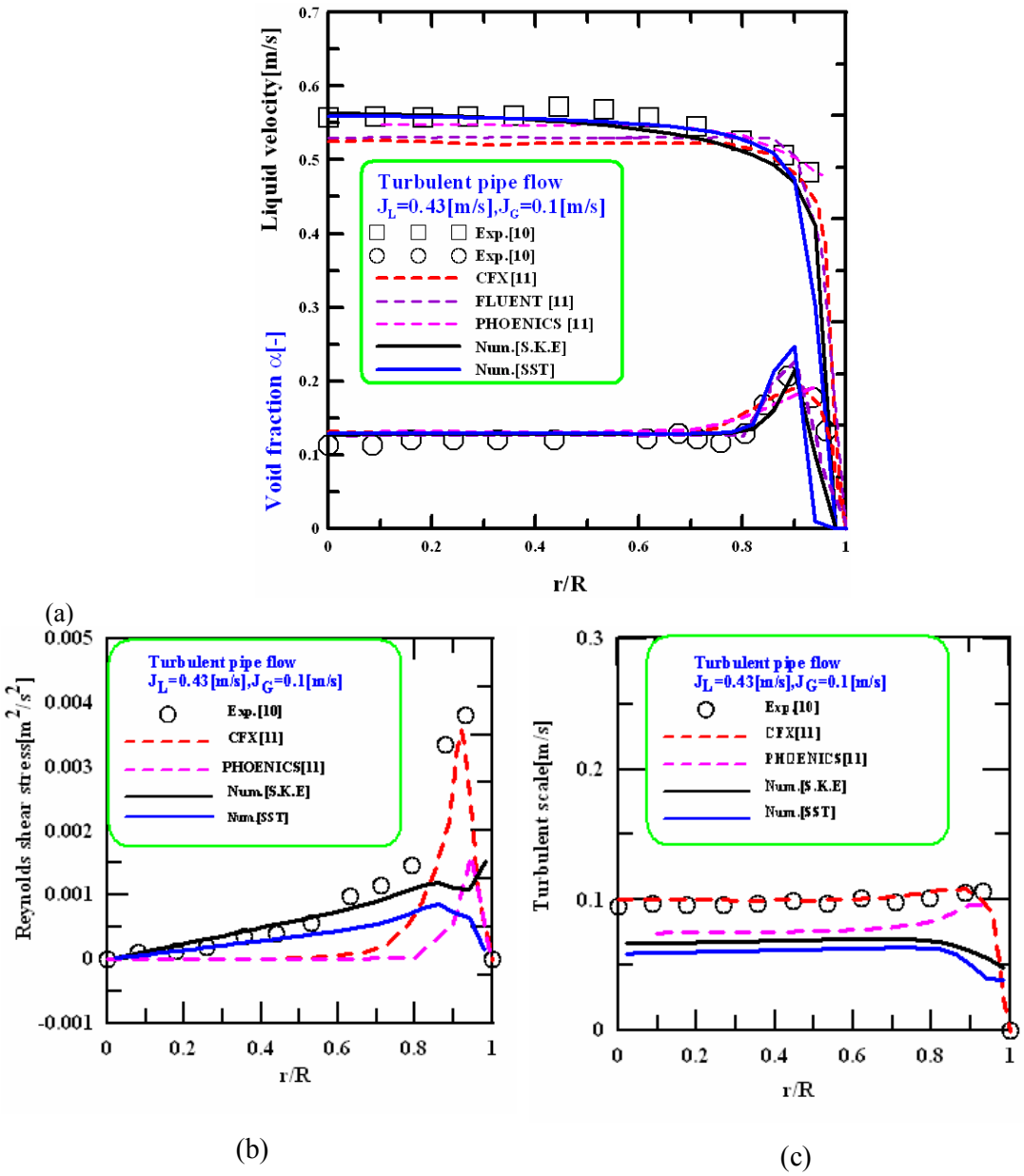

Figure 2 (a) Void fraction and liquid velocity, (b) Reynolds shear-stress, (c) r.m.s. liquid velocity, comparisons with case W1.

In fact, the present computations overestimate the stress magnitude in bubble-dominated regions for W3 case, while a reasonable agreement with experiments in case W2. As shown in Fig. 3(c) the predicted turbulence intensity is in a reasonable agreement with experiments. However, the numerical results drawn for the present turbulence models over predict the turbulence intensity for W3 as shown in Fig.4(c).

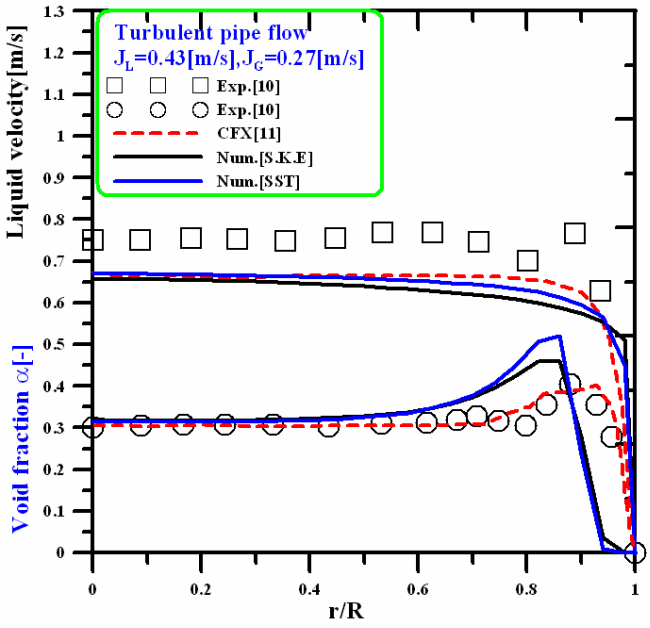

(a)

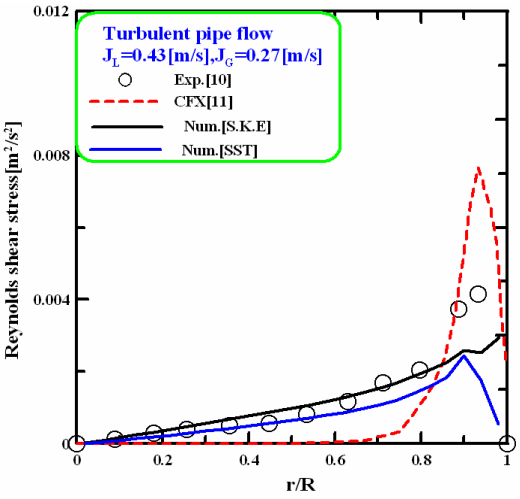

(b)

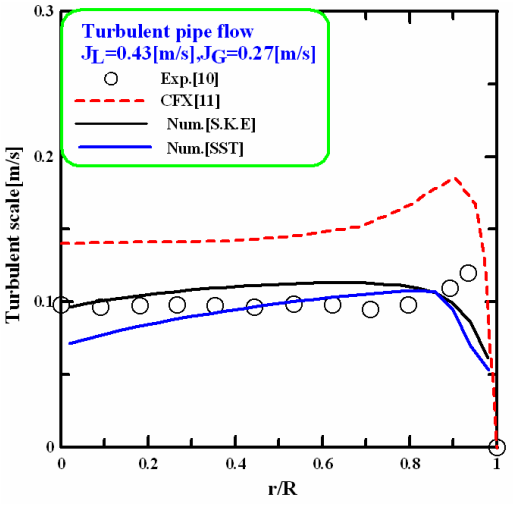

(c)

Figure 3 (a) Void fraction and liquid velocity, (b) Reynolds shear-stress, (c) r.m.s. liquid velocity, comparisons with case W2.

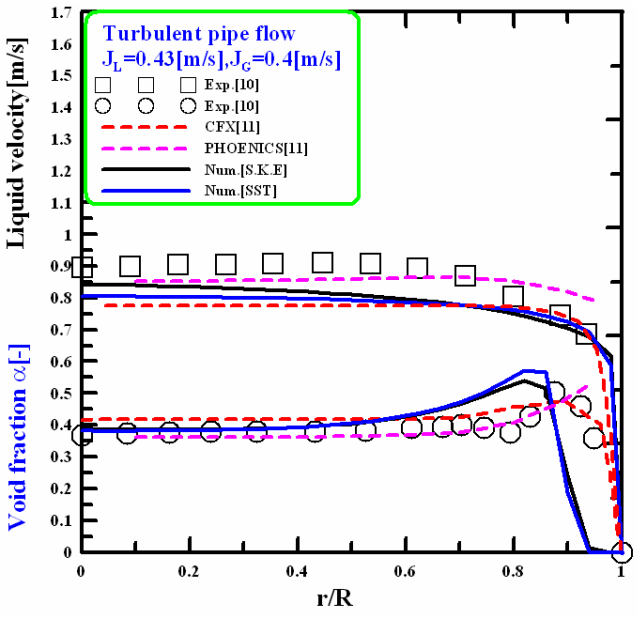

(a)

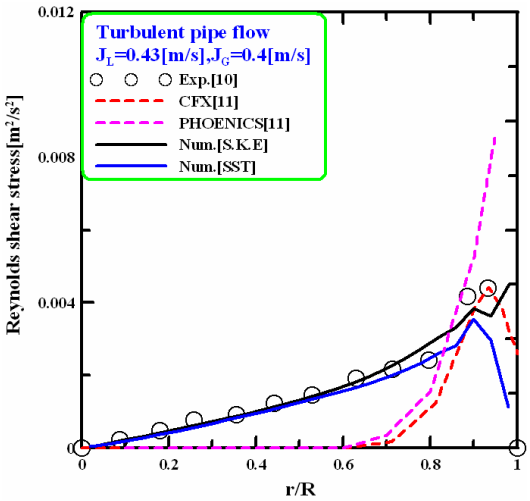

(b)

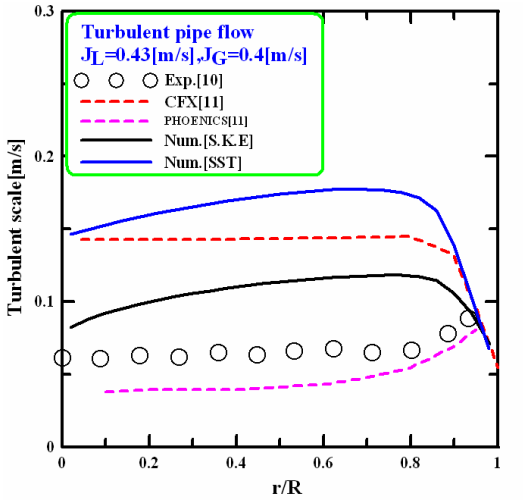

(c)

Figure 4 (a)Void fraction and liquid velocity, (b)Reynolds shear-stress, (c) r.m.s. liquid velocity, comparisons with case W3.

4.2. Sudden Enlargement in a Circular Pipe

The streamfunction for the two phase mixture Ψ_M is normalized by the total (liquid plus gas) inlet flow rate and is arbitrarily set to zero at the symmetry axis. The representation of the streamlines is then plotted in Fig.5 (a), in which the recirculation zone in the corner is clearly visible.

The turbulent viscosity μ_t is shown in Figs. 5(b). It is noticeable that most of the turbulent diffusion is produced far away from the enlargement. This is due to bubble-induced turbulence, which is represented by the additional two-phase source terms in the turbulence models equations.

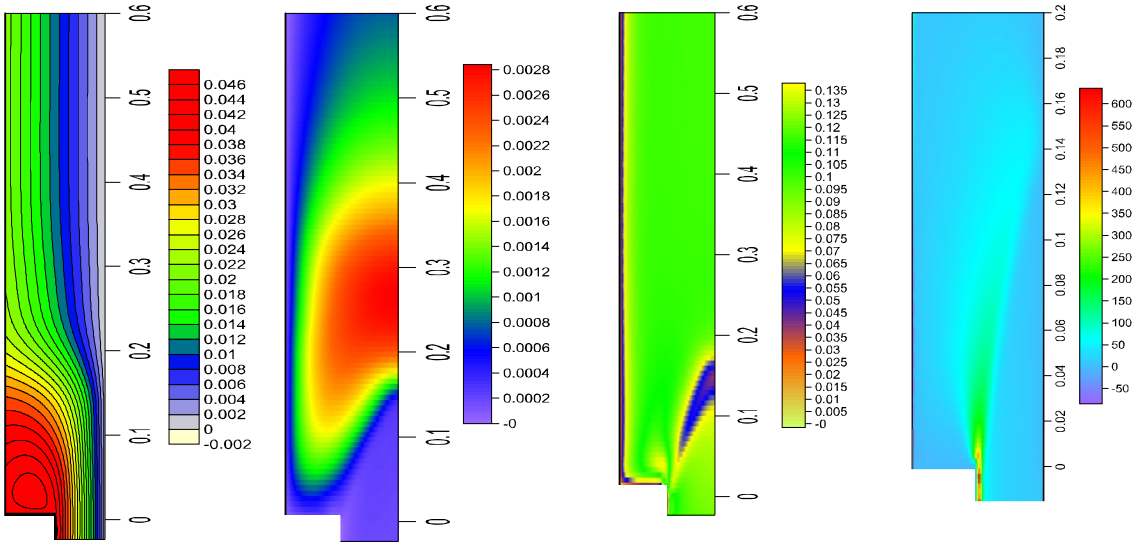

(a)Mixture streamlines (b)Turbulent viscosity (c)Gas phase fraction (d)Vorticity

Figure 5 Prediction for the sudden expansion flow:
(a) mixture streamlines, (b) turbulent viscosity contours, (c) void fraction contours and (d) vorticity contours.

In Fig. 5(c), the distribution of the gas phase fraction is pictured. As shown, the gas phase fraction is high close to the wall of the small pipe section and diffuses slowly further downstream. The accumulation of bubbles at the wall is characteristic for certain vertical pipe flows and is often referred to as a "wall peak" distribution. Its prediction remains a difficult task because of the coupled effects of shear, wake phenomena and deformation on the lift force as well as the turbulence of the liquid phase. In the region just behind the enlargement the gas phase fraction is very small, since the recirculation is not strong enough to drag bubbles back towards the enlargement and in this way to support an accumulation of bubbles in this region. This shows the effectiveness of using the phase-intensive momentum equations instead of standard ones for cases where one of the phases is not present locally. The distribution of vorticity contour is presented in Fig.5 (d). The shear layer in the separation zone and the elongation in the downstream of the step is also shown.

Profiles of the axial liquid velocity at five cross-sections: x=7, 13, 18, 25 and 32 cm downstream of the step wall of the sudden enlargement are shown in Fig.6. For the dilute C_t - model (Isaa and Oliveira [16]), the velocity difference generated by the enlargement is quickly diffused further downstream at x=25 cm, in which the predicted profile is almost uniform over the pipe radius. These results are not in agreement with the experimental data, but generally predictions using the experiential correction C_t – formulation by Behzadi et al. [14] improve the results. Here, the agreement between the calculation and the experimental data is good. In Figure 7, the results of the gas phase fraction field are shown. The peak at the first measuring location (x=7 cm) originates from an accumulation of bubbles at the wall of the small pipe section. The dilute Ct-formulation overpredicts the accumulation of bubble shortly behind the recirculation zone at x=7 cm. Although the profile at x=32 cm is predicted correctly by the dilute model of Isaa and Oliveira [16], the experimental data upstream shows a slower replenishment (renewal) on the centerline. In fact, the calculated centerline phase fraction diminishes between x=7 and 18 cm before it recovers rapidly between x=18 and 25 cm. With the Behzadi model [14], the phase fraction profiles are better predicted at stations close to the inlet, but discrepancies with the experimental data increase towards the outlet of the pipe.

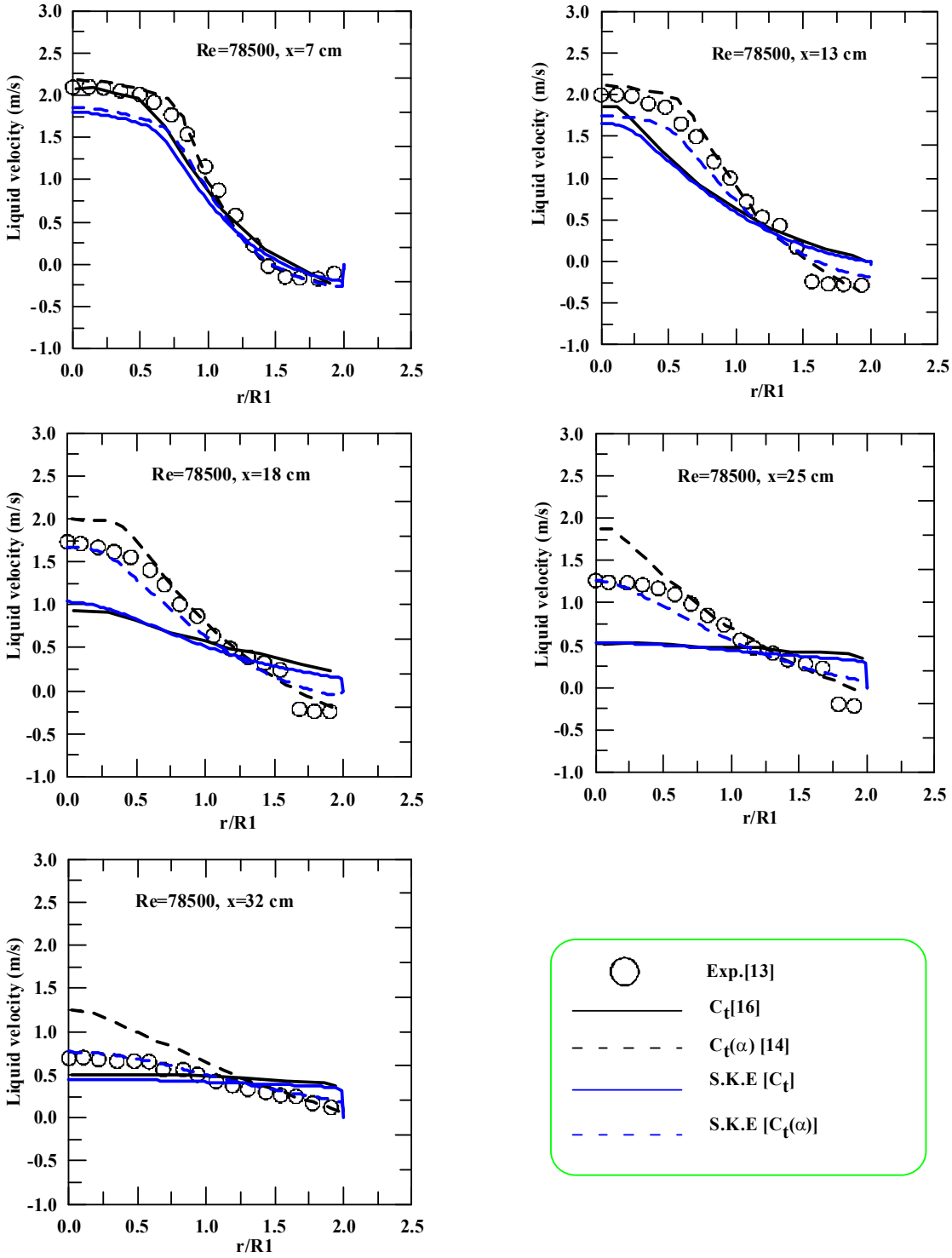

Figure 6 Continuous phase velocity profiles obtained from Issa and Behzadi model compared with experiment.

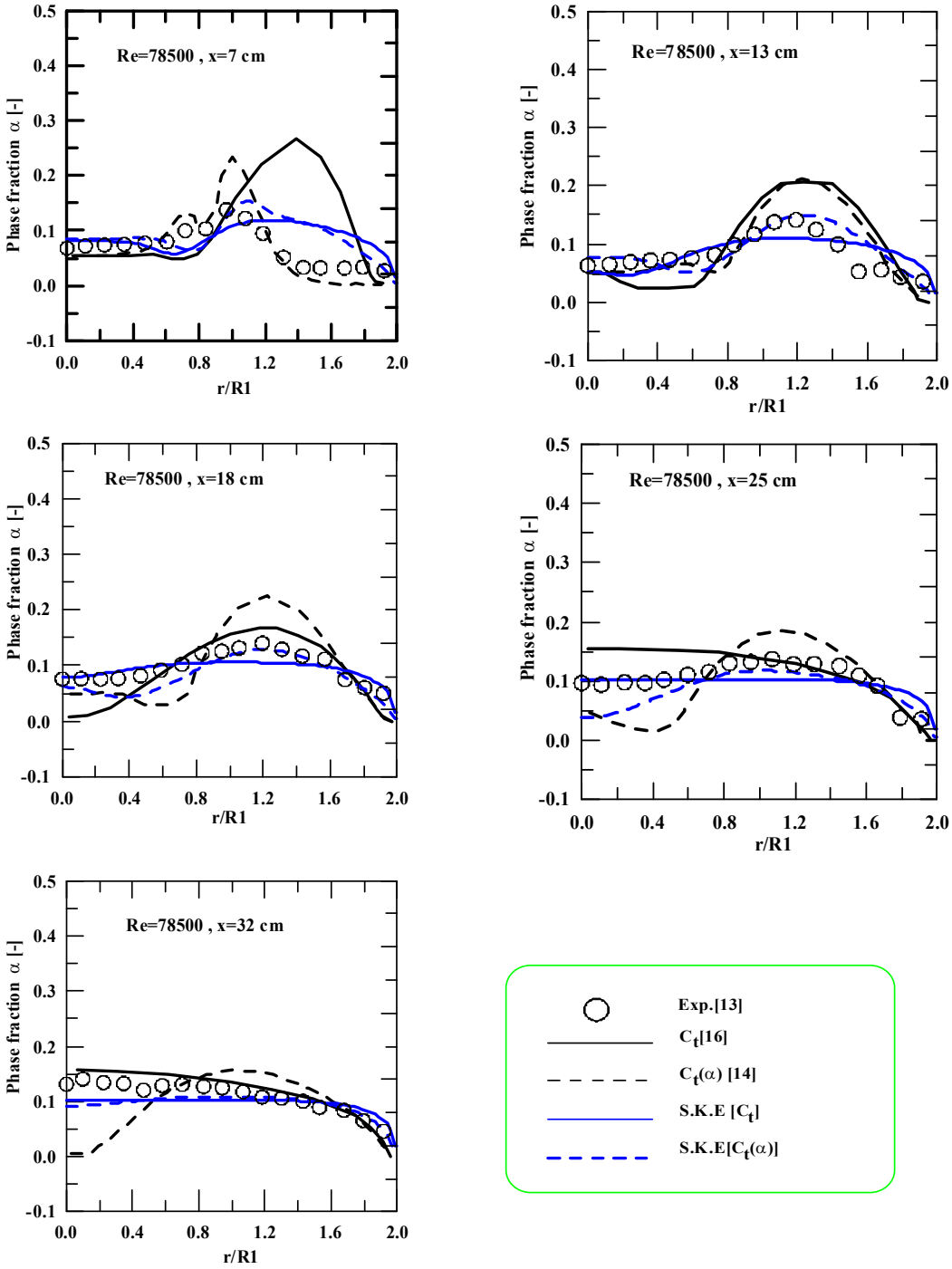

Figure. 7 Phase fraction profiles obtained from Issa and Behzadi model compared with experiment.

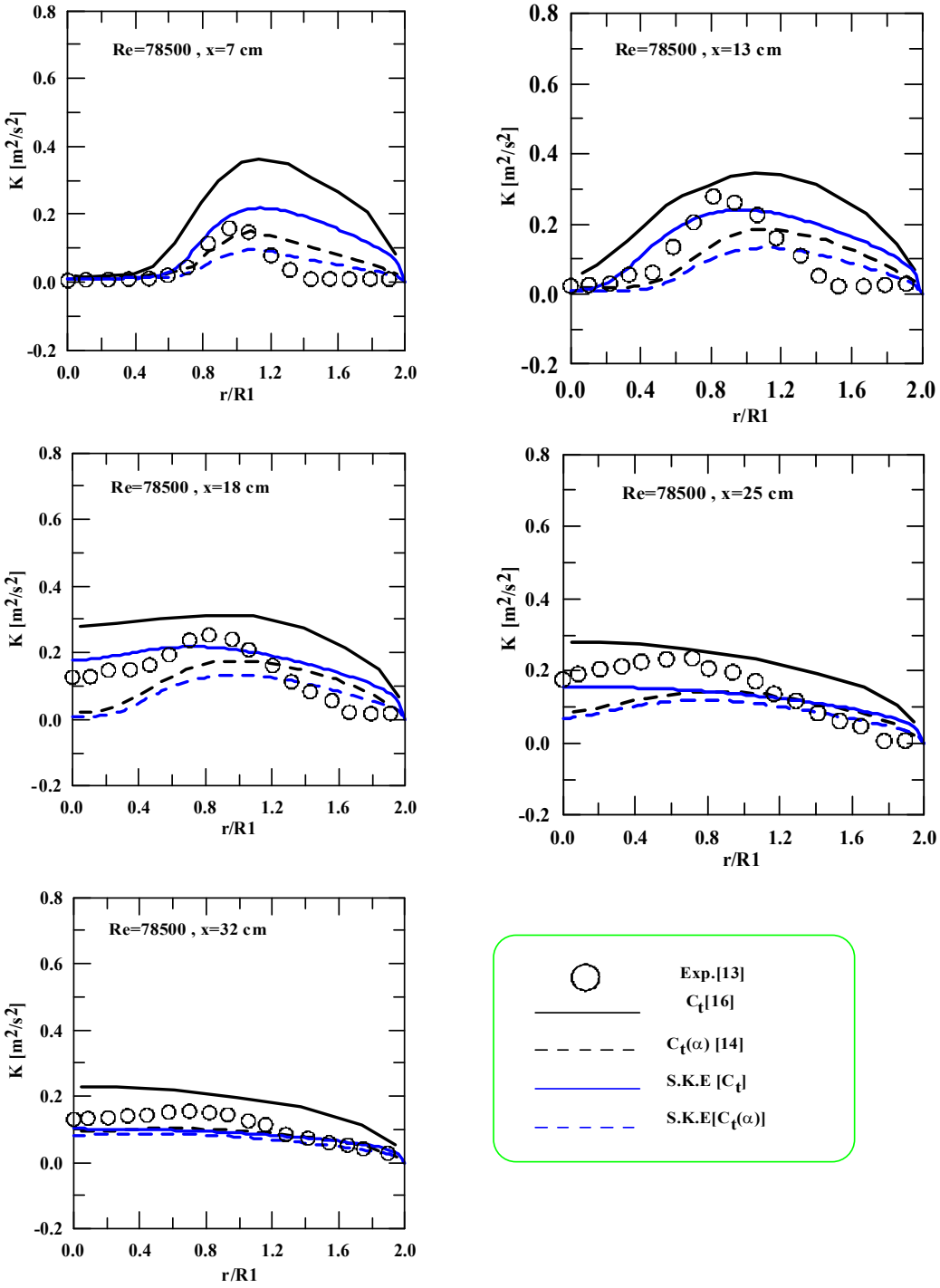

Figure. 8 Turbulence kinetic energy profiles obtained from Issa and Behzadi models compared with experiment.

Turbulent kinetic energy profiles are shown in Fig. 8. A significant improvement is obtained with the Behzadi model throughout the flow, which predicts a lower level of turbulent kinetic energy compared the overprediction of the dilute model (Isaa and Oliveira [16]).
However, Isaa model gives improvements in some different sections. The overall reduction of the kinetic energy is expected for rang of α values in this test case because C_t is close to unity

thereby diminishing the two-phase turbulence production term in source term in turbulence model equation.

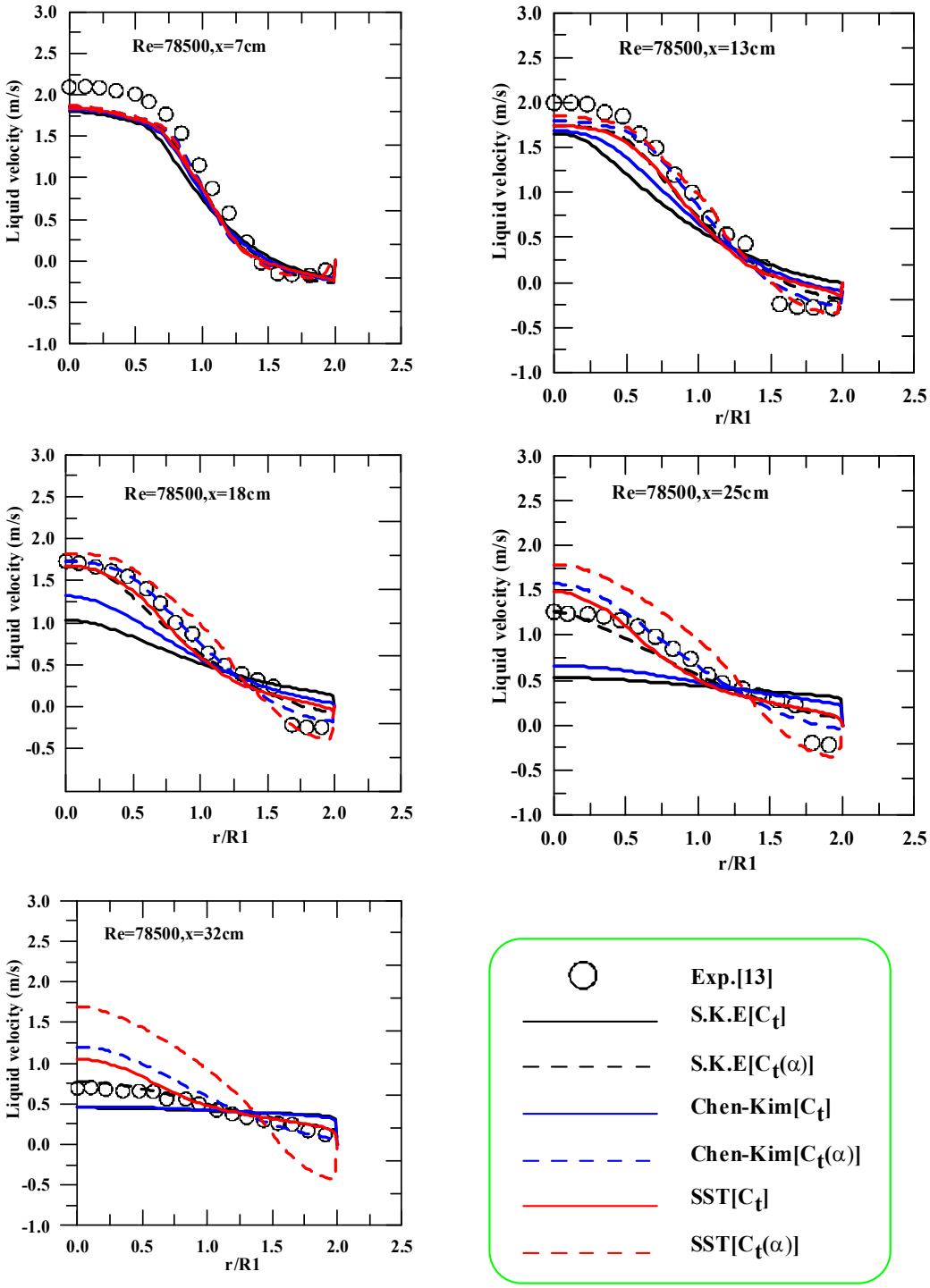

Figure. 9. Continuous phase velocity profiles obtained from Issa and Behzadi models compared with experiment.

In Figure 9, the results for the axial velocity field are shown by using different turbulence models with Behzadi and Issa modelling of C_t .

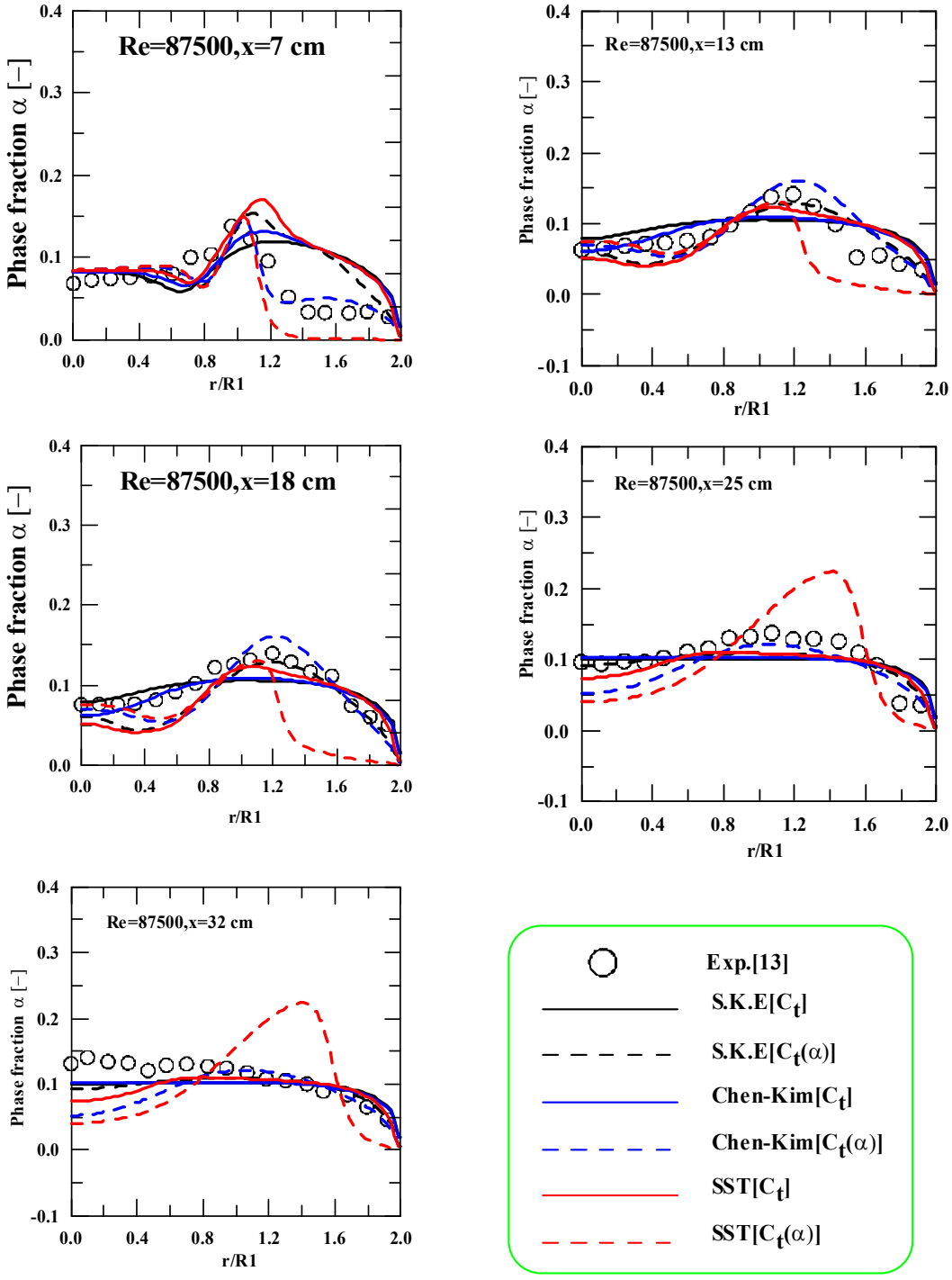

Figure. 10. Continuous phase velocity profiles obtained from Issa and Behzadi models compared with experiment.

These results are better predicted at station close to the inlet but the discrepancies with the experimental data increase in the streamline direction, but it is found that SST model with Issa model of C_t is better compared with other turbulence models at all stations.

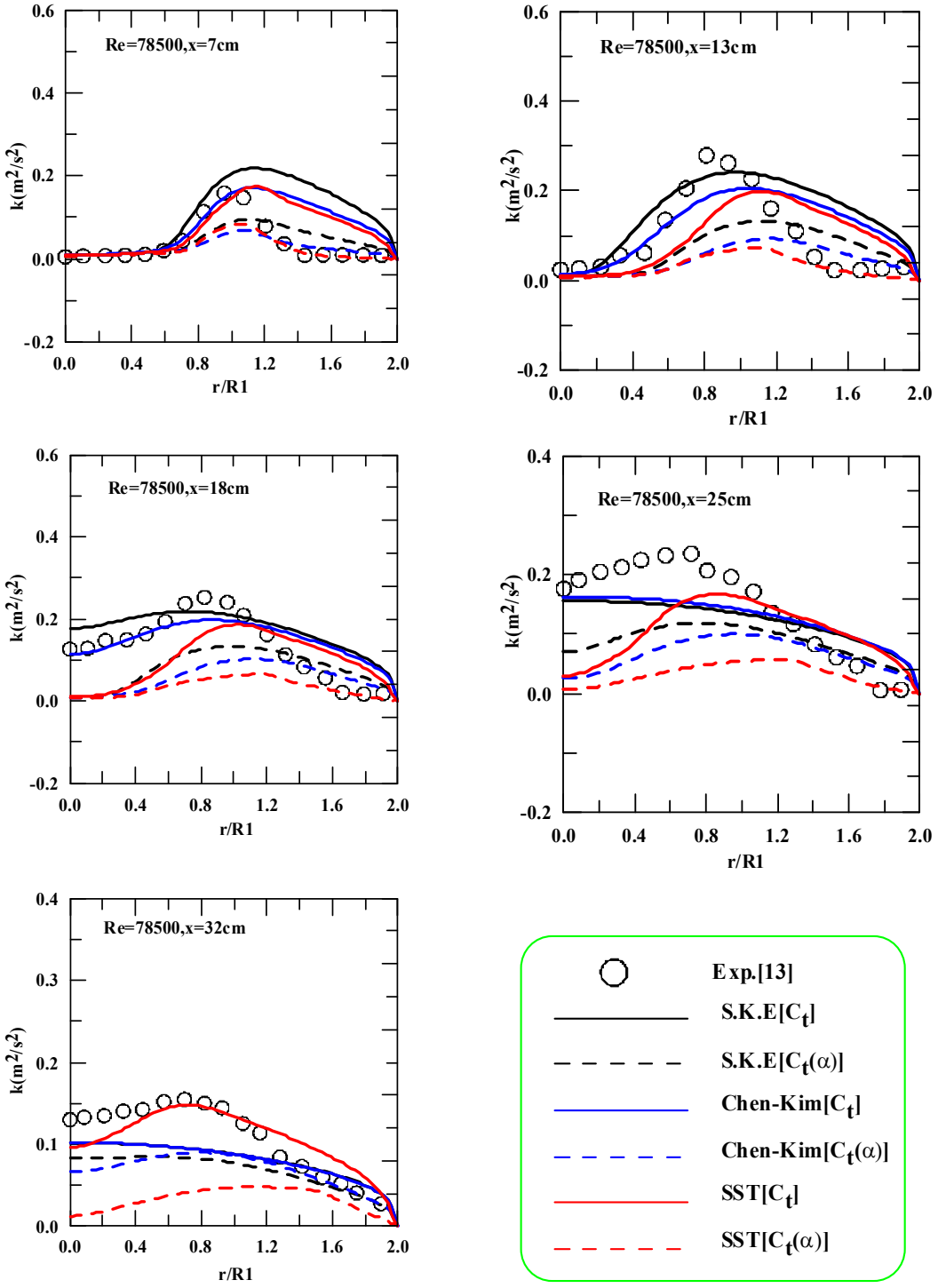

Figure. 11. Continuous phase velocity profiles obtained from Issa and Behzadi models compared with experiment.

The results for the phase fraction field are shown in Fig. 10 by using different turbulence model with Behzadi and Issa models of C_t. It is clear that SST model with Issa model of C_t is better compared with the other turbulence models at all station. Figure 11 shows the results for the turbulent kinetic energy by using different turbulence models with Behzadi and Issa modelling of C_t. Generally, SST model still plays an important role in simulating bubbly flow in view of the turbulence kinetic energy predictions. However, it is essential to highlight the limitations of the current turbulence model.

These limitations include the non-uniform distributions of the bubble sizes in the measurements. Also, the strong interaction between bubbles and sometimes slugs can be generated in the experiments and such phenomenon can not explicitly be predicted or considered in the turbulence models.

5. Conclusions

An Eulerian–Eulerian two fluid model for the prediction of dispersed two–phase (gas/liquid) flow at high volume fractions of the dispersed phase has been presented. A different turbulence models have then been implemented in a CFD code developed and tested for bubbly flow through a pipe and a pipe sudden expansion. Results for the continuous phase velocity, the phase fraction and turbulent kinetic energy using Isaa C_t model and Behzadi C_t model have been presented. The results showed some improvement in the Behzadi C_t model over the Isaa C_t model but not at all computational domain because of the absence of the inflow turbulence specifications. It is concluded however, that the turbulence models need more improvements to account more accuracy for bubble induced turbulence. The improvements can consider detailed bubble interactions during bubble collapse and coalescence. Also, there are some limitations of using Eulerain-Eulerain two-fluid model for predicting gas phase should be considered.

References

[1] M. Ishii, Thermo-fluid dynamic theory of two-phase flow, Eyrolles, Paris, (1975).

[2] R.L.Gudmundsson, On stability of solutions to the two-phase models for dispersed two-phase flow, Royal Institute of Technology, Stockholm, (2002) (Report)

[3] O.Simonin and P.L.Viollet, Numerical study on phase dispersion mechanism in turbulent bubbly flows, Int. Conf. on Mechanics of Two-Phase Flows, June (1989) 12–15,Taipei, Taiwan.

[4] S. J. Lee, Jr.R.T. Lahey, and Jr. O. C. Jones, "The prediction of two phase turbulence and phase distribution phenomena using k-ε model", Jap. J. Multiphase Flow 3(1989) 335–368.

[5] M. Lopez de Bertodano, S. J. Lee, R.T. Lahey and D.A. Drew, The prediction of two-phase turbulence and phase distribution using a Reynolds stress model, J. Fluids Eng. 112(1990) 107–113.

[6] R. Bel Fdhila and O. Simonin, Eulerian prediction of a turbulent bubbly flow downstream of a sudden pipe expansion, Workshop on two-phase flow predictions, 30 March–2 April, Erlangen (1992).

[7] M. Lopez de Bertodano, S.J. Lee, R.T. Lahey and O.C. Jones, Development of a k-ε model for bubbly two-phase flow, J. Fluids Eng. 116(1994) 128–134.

[8] M.A. Lopez de Bertodano, Turbulent bubbly two-phase flow in a triangular duct,Ph.D. dissertation, Rensselaer Polytechnic Institute, (1992).

[9] Y. Sato, M. Sadatomi and K. Sekoguchi, Momentum and heat transfer in two-phase bubble flow, Part I and II, Int. J. Multiphase Flow 7(1981) 167-190, 1981.

[10] S.K. Wang, S.J. Lee, O.C. Jones and R.T. Lahey, 3D turbulence structure and phase distribution measurements in bubbly two-phase flows, Int. J. Multiphase Flow, 13(3) (1987) 327-343.
[11] A.A.Troshko and Y.A. Hassan,A two-equation turbulence model of turbulent bubbly flows, Int. J. Multiphase Flow, 27(2001) 1965-2000, 2001.
[12] A.D. Gosman, R.I. Issa, C. Lekakou, M.K. Looney and S. Polities, Multidimensional modeling of turbulent two-phase flows in stirred vessels, The American Institute of Chemical Engineers Journal 38(12)1(1992)1946-1956.
[13] R. Bel F'dhila, Analyse experimental et modeisation d'un ecoulement vertical a bubbles dan un elargissement brusque, Ph.D. Thesis, Institute National Polytechnique de Toulouse (1991).
[14] A. Behzadi, R.I. Issa and H. Rusche, Modelling of dispersed bubble and droplet flow at high phase fractions, Chemical Engineering Science 59(2004) 759 – 770.
[15] M.B. Carver, Numerical computation of phase separation in two fluid flow, Journal of Fluids Engineering. 106 (1984) 147-153.
[16] R. Issa and P. Oliveira, Numerical aspects of an algorithm for the Eulerian simulation of two-phase flows, Int. J. Numerical Method in Fluids, 43(2003) 1177-1198.
[17] K. Manmatha and K. Sukasnta, Two-phase pressure drop caused by sudden flow area contraction/expansion in small circular pipes, Int.J. Numerical Method in Fluids (2010).
[18] FB. Wallis, One-dimensional two-phase flow, McGraw-Hill: New York (1969).
[19] M. Ishii and N. Zuber, Drag coefficient and relative velocity in bubbly, droplet or Particulate flows, AICHE Journal, 25(1979) 843-855.
[20] S.P. Antal, Jr. R.T. Lahey and J.E. Flaherty, Analysis of phase distribution in fully developed laminar bubbly two-phase flow, International Journal of Multiphase Flow, 17 (1991) 635-652.
[21] Y.S. Chen and S.W. Kim, Computation of turbulent flows using extended k-ε turbulence closure model, NASA contraction report, NASA CR-179204(1987).
[22] R. Florian Menter, Zonal two equation k-ω, turbulence models for aerodynamic flows, AIAA (1993) 93-2906.
[23] R. Florian Menter, Two-equation eddy-viscosity turbulence models for engineering applications, AIAA JOURNAL, 32, No. 8(1994).
[24] Guan Heng, Computational techniques for multi-phases flows, The Boulevard, Langford Lane, Kidlington, Oxford OX5 1GB, UK (2010).
[25] D.P. Hill, D.W. Wang, A.D. Gosman and R.I. Issa, Numerical prediction of bubble dispersion in shear layers, In: Third International Symposium on Multiphase Flow and Heat Transfer, Xian, China (1994) 110-117.
[26] C. Garnier, M. Lance and J.L. Marie, Measurements of local flow characteristics in buoyancy-driven bubbly flow at high void fraction, In: Michaelides, E.E., et al.(Eds.), Proceedings of the Fourth International Conference on Multiphase Flow, New Orleans, LA, USA, May 27–June 1(2001).
[27] A. Larue de Tournemine, V. Roig and C. Suzanne, Experimental study of the turbulence in bubbly flows at high void fraction, In: Michaelides, E.E., et al. (Eds.), Proceedings of the Fourth International Conference on Multiphase Flow, New Orleans, LA, USA, May 27–June 1(2001).
[28] F. Augier, Structure locale du champ hydrodynamqiue dans les ecoulements disperses liquide-liquide concentres, Ph.D. Thesis, Institut National Polytechnique de Toulouse (2001).
[29] M. Lance, J.L. Marie, E. Moursali, J. Bataille, C. Suzanne, V. Roig, R. Bel Fdhila, and L.Masbernat, Experimental study of turbulent bubbly shear flows, Chemical Engineering Communications (196)141–142, 51–70.
[30] H. Schlichting, Boundary layer theory, MeGraw-Hill (1979).
[31] SV.Patankar, Numerical heat transfer and fluid flow, Hemisphere Pub.: Washington, DC (1980).